Ning Zhou and Bryan E. Pfingst: JASA Express Letters [http://dx.doi.org/10.1121/1.4943783] Published Online 15 March 2016

Evaluating multipulse integration as a neural-health correlate in human cochlear-implant users: Relationship to forward-masking recovery

Ning Zhou
Department of Communication Sciences and Disorders, East Carolina University, Greenville, North Carolina 27834, USA
zhoun@ecu.edu

Bryan E. Pfingst
Kresge Hearing Research Institute, Department of Otolaryngology, University of Michigan, Ann Arbor, Michigan 48109-5616, USA
bpfingst@umich.edu

Abstract: The present study evaluated the slopes of threshold-versus-pulse-rate functions (multipulse integration, MPI) in humans with cochlear implants in relation to recovery from 300-ms forward maskers. MPI has been correlated with spiral ganglion cell density in animals. The present study showed that steeper MPI functions were correlated with faster recovery from forward masking. The findings suggested that the variations in the MPI slopes are explained not only by the quantity of neurons contributing to the integration process but also by the neurons' temporal response characteristics and possibly central inhibition.

[QJF]
Date Received: November 30, 2015 **Date Accepted:** February 29, 2016

1. Introduction

The present paper evaluates in human subjects with cochlear implants a psychophysical correlate of neural health that was established in guinea pig studies. The slope of the function relating threshold to pulse rate below 1000 pps for pulse trains of fixed duration has been shown to correlate significantly with the spiral ganglion neuron (SGN) density near the tested electrodes (Kang *et al.*, 2010; Pfingst *et al.*, 2011; Zhou *et al.*, 2015). The slope of the threshold versus pulse rate function is a measure of multipulse integration (MPI). Threshold improvement with the increase of pulse rate is believed to depend on whether there is sufficient neural representation for the increasingly narrow-spaced pulses in the stimulus (Zhou *et al.*, 2015). A number of factors could cause a high-rate stimulus to be under-sampled, which would reduce the difference between the neural representations of the high and low rate stimuli. The variable of neural survival is thought to contribute to MPI because having a high SGN density increases the number of excitable neurons for any pulse in the high-rate pulse train. In human subjects, the number of neurons that can be recruited for the integration process could also depend on the factor of electrode-neuron distance.

A second set of factors that could cause a high-rate stimulus to be under-sampled is the neural temporal properties, which could vary depending on pathology and/or site of neural excitation. Factors including refractoriness, adaptation, and central inhibition may all reduce neural responses at high rates, leading to a shallow multipulse integration function. In human and animal subjects without measurable residual hearing, the auditory nerve fibers respond to pulsatile stimulation in an alternating temporal pattern of high and low amplitudes in the pulse-rate range of 400–2000 pps (Wilson *et al.*, 1997; Hughes *et al.*, 2012; Ramekers *et al.*, 2015). This alternating pattern reflects the individual differences in the absolute and relative refractory period of the auditory neurons. If there are more auditory neurons with a relatively short refractory period, it is more likely that each pulse in the high-rate stimulus will be represented. Besides refractoriness, neural responses will reduce over the course of the high-rate pulse train due to either nerve or central adaptation (Boulet *et al.*, 2016). If there were less adaptation in the neural responses, greater integration would also occur. Animal studies have shown that in short-term deafened mice, the surviving auditory neurons have significantly prolonged refractory periods compared to those in hearing ears (Zhou *et al.*, 1995), and the effect of deafness may be even larger with long-term

nerve degeneration (Miller *et al.*, 2010). It is likely that in deafened human ears, the neural temporal response properties vary across stimulation sites and ears due to differences in pathology.

Several of the factors related to temporal response properties of neurons should be manifested in the shape of the forward-masking recovery function. A rapid recovery component directly related to refractoriness could be followed by a second slow recovery component related to nerve or central adaptation (Nelson and Donaldson, 2001; Chatterjee, 1999). The slow component, if it never completely recovers, results in residual masking and is thought to reflect a central inhibition mechanism (McKay, 2012). If the MPI slope is related to these factors, it would be correlated with the time constants of one or more components of the forward-masking recovery function. Depending on the strength of the relationship between MPI and the various recovery components, the results could provide insights into whether, besides SGN density, MPI might be used to estimate heath of the surviving neurons in the implanted cochlea.

2. Methods

2.1 Subjects and hardware

Eight post-lingually deafened adult subjects participated in the study, and one of the subjects who had bilateral implants (S99) was tested in both ears. The nine tested ears used Nucleus CI24RE or CI512 devices. Cochlear implant use ranged from 1.2 to 7.8 yr (mean $\pm$ sd, 3.38 ± 2.33) at the time of data collection. Duration of deafness (onset of profound hearing loss to implantation) ranged from 2.5 to 64.1 yr (mean $\pm$ sd, 23 ± 21.65). None of the subjects had measurable residual hearing in the tested ear or the non-implanted ear. The use of human subjects for this study was reviewed and approved by the University of Michigan Medical School Institutional Review Board and East Carolina University Institutional Review Board.

2.2 Psychophysical testing

Laboratory-owned Freedom processors (Cochlear Corporation, Englewood, CO) were used for the psychophysical tests. The stimuli were delivered through MATLAB programs that bridged with the NIC II research interface. The psychophysical tests used trains of symmetric biphasic pulses with a phase duration of 25 μs and an interphase interval of 8 μs, presented in a monopolar (MP 1 + 2) electrode configuration.

For each stimulation site, psychophysical detection thresholds were measured for two pulse rates (80 and 640 pps) with a fixed pulse-train duration of 250 ms. Pulse rates were kept below 1000 pps because MPI slopes that were most strongly correlated with the cochlear health factors were those for pulse rates below 1000 pps (Pfingst *et al.*, 2011). Detection thresholds were determined using the method of adjustment. Subjects were instructed to use the three sets of buttons in a graphic user interface on the computer screen; this allowed up- and down-changes in 25, 5, and 1 clinical level unit (CLU) steps. To reduce the effect of tinnitus on stimulus detection, subjects were instructed to raise the level of the stimulus such that it produced a loudness that the subject could confidently detect and then decrease it to the level that was barely audible. Previous studies have shown that the method of adjustment and adaptive tracking methods yielded very similar results in these subjects (e.g., Zhou *et al.*, 2015). For each pulse rate, two thresholds were estimated and the average was taken. The thresholds were first converted from CLU to dB re 1 mA, and MPI slopes were defined as the rate of threshold decrease in decibels per doubling of pulse rate. Of all stimulation sites, two sites, one with a steep MPI slope and one with a shallow MPI slope, were selected and measured for forward-masking recovery. For three of the subjects (S60R, S89R, S69L), two pairs of sites with relatively steep and shallow MPI slopes (four sites) were measured for forward-masking recovery. One pair was used for other subjects.

In measuring forward-masking recovery, the masker was 300 ms long and was always presented at the same electrode as the probe, which was 20 ms long. The pulse rate was 900 pps. The level of the maskers was loudness balanced to the loudness at 50% of the dynamic range (DR) of the probe. Probe delay (offset of the masker to the onset of probe) was set at 1, 4, 7, 10, 20, 50, 100, or 200 ms, although in some subjects, some of the shorter probe delays were not tested due to time constraints. Threshold of the probe was first obtained without the masker and then in the presence of the masker with varying probe delays using a three-interval forced-choice (3IFC) paradigm. The probe level started at 50% DR and was adapted using a 2-down 1-up rule. The forward-masking recovery was quantified as probe threshold elevation in decibel versus

log probe delay, and probe threshold elevation in microamperes versus probe delay. Each function was normalized to the respective threshold elevation at 1 ms probe delay. Representing forward-masking recovery on a log-log scale removes any confounding effects of unmasked probe threshold on the amount of forward masking (McKay, 2012), whereas plotting forward-masking recovery in linear units makes it possible to derive time constants of various recovery components if a multiple-component pattern exists. The log-log recovery function was fit with a single slope. When recovery was plotted on linear axes, two recovery components were often observed, consistent with previous studies that used long forward maskers (e.g., Chatterjee, 1999). Thus the two decay exponential components were fit with a fast time constant $\tau 1$ and a slow time constant $\tau 2$. The discontinuity of the function, where the first and second exponential transitioned, was visually inspected. When the discontinuity was ambiguous, the break point that produced the best fit was determined. The last data point in the rapid recovery component was included in the fitting for $\tau 2$, if that produced less fitting error.

3. Results

Figure 1 shows the forward-masking recovery functions plotted on a log-log scale. A single line was fit to each of these functions although some functions could be better described with multiple slopes. The slopes of these single lines did not correlate with the MPI slopes [r (23) = 0.27, $p = 0.2$]. The recovery process was also described on linear scales with two time constants (Fig. 2). The two-exponential pattern was very evident for some stimulation sites but less prominent for others, consistent with the first-order discontinuities shown in Fig. 1. The probe delays used as the boundary for fitting the two exponentials ranged from 7 to 50 ms. The fast-recovery time constant fit from the first component ($\tau 1$) ranged from 10.54 to 151.87 ms (mean ± sd, 53.6 ± 35). Slopes of the MPI functions were predicted by the time constant $\tau 1$ [r (23) = 0.51, $p = 0.01$] (Fig. 3, left panel). Faster recovery, i.e., smaller recovery time constants, predicted

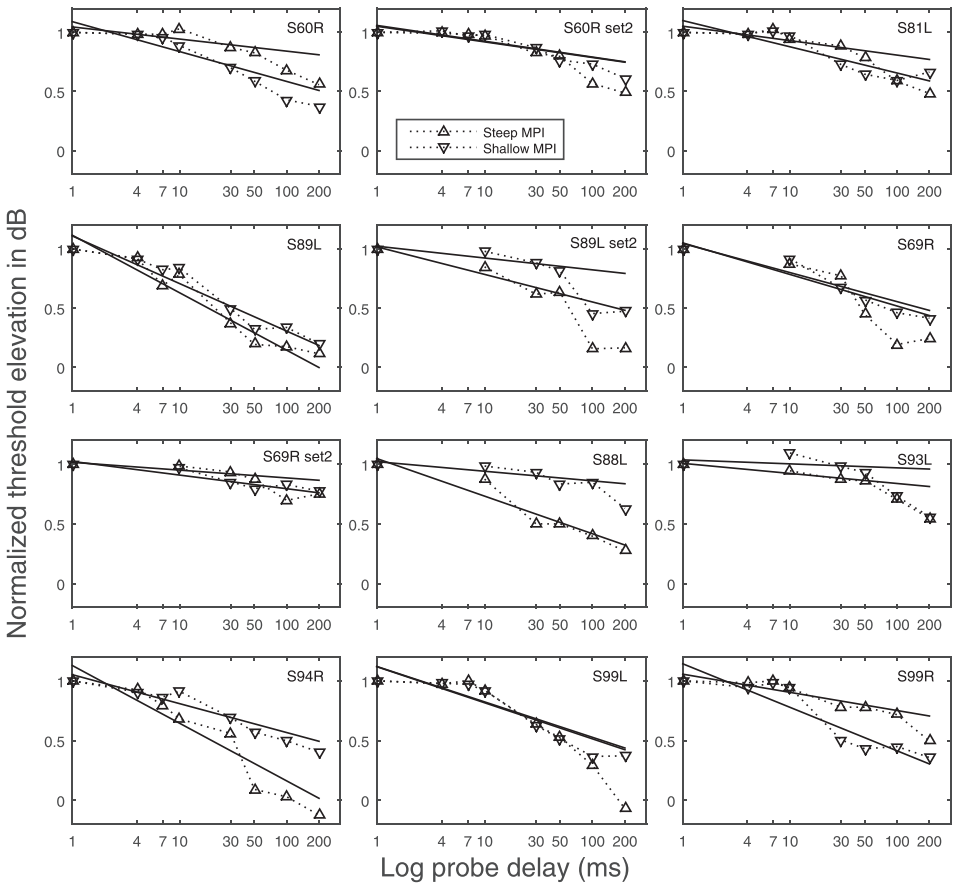

Fig. 1. Normalized forward-masking recovery functions on log-log scales. Normalized threshold elevation in decibels is plotted against the log time delay between the masker and probe (triangles connected by dashed lines). The up-pointing triangles are data measured at the stimulation sites with steep MPIs, whereas the down-pointing triangles are data measured at the stimulation sites with shallow MPIs. Each function was fit with a straight line.

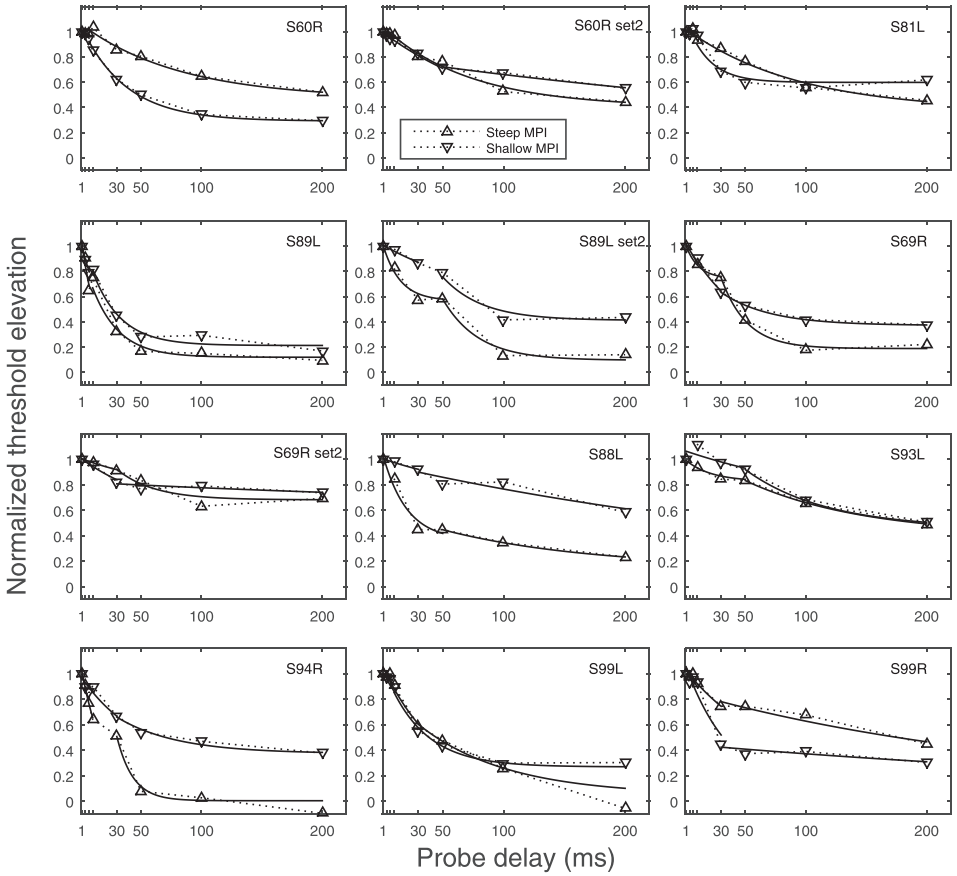

Fig. 2. Normalized forward-masking recovery functions on linear scales. Normalized threshold elevation in microamperes is plotted against the linear time delay between the masker and probe (triangles connected by dashed lines). The up-pointing triangles are data measured at the stimulation sites with steep MPIs, whereas the down-pointing triangles are data measured at the stimulation sites with shallow MPIs. Each curve was fit with two exponentials and the fitting was plotted as solid lines.

steeper MPI slopes. The slow-recovery time constant from the second component ($\tau 2$) ranged from 13.34 to 497.74 ms (mean $\pm$ sd, 128.24 $\pm$ 161.99). The time constants fit to the second component of the recovery function ($\tau 2$) did not have a statistically significant relationship with the MPI slopes [r (23) = 0.28, $p = 0.18$] (Fig. 3, middle panel). At most of the tested stimulation sites, threshold did not completely recover from forward masking, even at the longest probe delay of 200 ms. The residual forward masking, i.e., threshold elevation at the 200 ms probe delay, was significantly correlated with the MPI slopes [r (23) = 0.48, $p = 0.018$] (Fig. 3, right panel); greater residual masking predicted shallower MPI slopes.

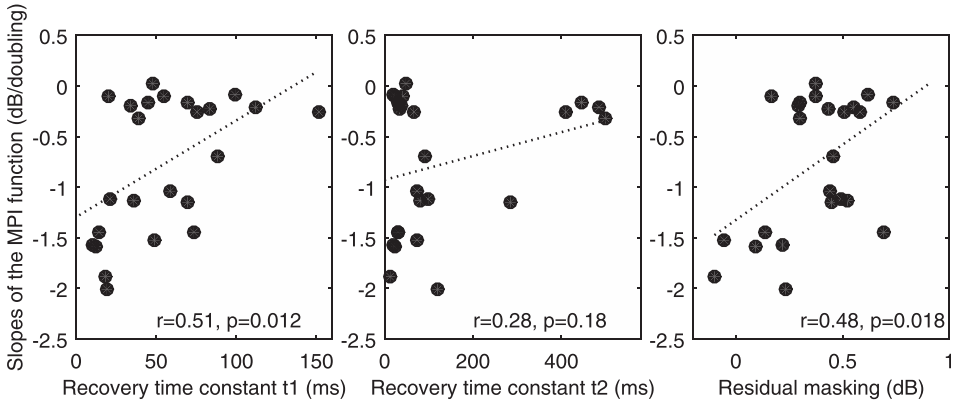

Fig. 3. Scatter plots of the MPI slopes against forward-masking recovery time constants (left and middle panels) and residual masking (right panel). Each data point represents one stimulation site ($n = 24$). The dashed lines show linear fits to the data. Correlation coefficients and p values are shown in each panel.

4. Discussions and conclusion

Data from the present study are consistent with the hypothesis that the MPI slopes are related to the peripheral neural temporal response properties, supported by findings that greater multipulse integration was associated with faster recovery of the early-recovery component following forward masking. The relationship between the MPI slopes with residual masking at 200 ms after the masker offset indicates that some of the variance in MPI might also be explained by central inhibition.

Given that the duration of the masker used was long, several possible recovery processes are likely involved, i.e., the recovery from refractoriness, neural adaptation, and possibly recovery from central inhibition. In acoustic hearing, the origin of forward masking at the long probe delays was thought to be due to depletion of neurotransmitters in the hair-cell auditory-neuron synapse (Smith and Brachman, 1982; Westerman and Smith, 1984). However, electrically evoked compound action potentials (ECAPs) measured in animals with deafened cochleae without hair cells indicated that the origin of adaptation could well be at the level of the eighth nerve (Killian *et al.*, 1994). There is also evidence to indicate that the origin of adaptation could be central to the auditory nerve. First, the forward masking functions observed in brain stem implant patients were found to be similar in pattern compared to those measured in normal-hearing listeners, suggesting that the mechanism of adaption could reside at retro-cochlear locations (Shannon, 1990). In addition, Nelson and Donaldson (2001) observed that in some cochlear implant subjects, a single-pulse forward masker could produce a recovery pattern with a fast time constant of a few milliseconds that is related to refractoriness and a second slow and sometimes incomplete recovery component. They suggested that the slow component indicates recovery from central adaptation.

Forward-masking recovery on the log-log scale showed more than one slope in many cases, and the slopes of the single lines fit to these functions did not correlate with the MPI slopes. The recovery functions were examined further on linear scales where a two-exponential pattern and sometimes a more smooth decay with probe delays was seen; both patterns have been reported in previous studies that used long maskers (Chatterjee, 1999; Nelson and Donaldson, 2002). Chatterjee (1999) demonstrated that when a two-exponential pattern was present, the relative dominance of the slow and fast recovery components varied with the duration of the masker. A discontinuity in the function might suggest the completion of recovery of refractoriness and nerve adaptation for example, and the start of recovery from central inhibition. A smooth function might suggest the overlap of recovery in these variables. For simplicity of data analysis, all functions were fit with two exponentials. The mean (54 ms) and range (11–152 ms) of the fast time constants were comparable to what was reported previously in forward masking experiments using long maskers (e.g., Nelson and Donaldson, 2002). The fast time constant likely reflected a combined effect of recovery from refractoriness and nerve adaptation because it was considerably longer than what would be expected from a single process of recovery from refractoriness, which typically occurs within a few milliseconds (Stypulkowski and van den Honert, 1984). Consistent with the previous findings (Chatterjee, 1999; Nelson and Donaldson, 2001, 2002), for most stimulation sites, probe thresholds did not recover with the longest probe delay tested, i.e., 200 ms, and the amount of residual masking was also correlated with the MPI slopes. The mechanism of residual masking is thought to be central (Oxenham and Moore, 1994; McKay, 2012), thus it seems possible that central factors as well as auditory-nerve properties constrain multipulse integration.

Psychophysical forward-masking recovery functions have been shown to correlate with whole nerve action potential refractory recovery functions (Brown *et al.*, 1996) as well as with word recognition (Nelson and Donaldson, 2001). These results echo our recent finding that the MPI slopes, which the current data suggest reflect temporal characteristics of the auditory nerve, predicted sentence, and phoneme recognition in noise (Zhou and Pfingst, 2014).

Previous studies showed that, in guinea pigs, the MPI slopes were correlated with neural density near tested stimulation sites (e.g., Kang *et al.*, 2010; Pfingst *et al.*, 2011; Zhou *et al.*, 2015). Evidence from the current study suggests that the MPI slopes might also reveal the temporal response properties of the surviving neurons. It might be that the SGN density and temporal properties of the neurons co-vary in implant subjects, but that hypothesis remains to be tested.

Acknowledgment

We thank our dedicated cochlear implant subjects for their participation. This work was supported by NIH-NIDCD Grant Nos. R01 DC010786 and P30 DC05188 and an Emerging Research Grant from the Hearing Health Foundation.

References and links

Boulet, J., White, M., and Bruce, I. C. (**2016**). "Temporal considerations for stimulating spiral ganglion neurons with cochlear implants," J. Assoc. Res. Otolaryngol. **17**, 1–17.

Brown, C. J., Abbas, P. J., Borland, J., and Bertschy, M. R. (**1996**). "Electrically evoked whole nerve action potentials in Ineraid cochlear implant users: Responses to different stimulating electrode configurations and comparison to psychophysical responses," J. Speech Hear. Res. **39**, 453–467.

Chatterjee, M. (**1999**). "Temporal mechanisms underlying recovery from forward masking in multielectrode-implant listeners," J. Acoust. Soc. Am. **105**, 1853–1863.

Hughes, M. L., Castioni, E. E., Goehring, J. L., and Baudhuin, J. L. (**2012**). "Temporal response properties of the auditory nerve: Data from human cochlear-implant recipients," Hear. Res. **285**, 46–57.

Kang, S. Y., Colesa, D. J., Swiderski, D. L., Su, G. L., Raphael, Y., and Pfingst, B. E. (**2010**). "Effects of hearing preservation on psychophysical responses to cochlear implant stimulation," J. Assoc. Res. Otolaryngol. **11**, 245–265.

Killian, M. J. P., Klis, S. F. L., and Smoorenburg, G. F. (**1994**). "Adaptation in the compound action potential response of the guinea pig VIIIth nerve to electrical stimulation," Hear. Res. **81**, 66–82.

McKay, C. M. (**2012**). "Forward masking as a method of measuring place specificity of neural excitation in cochlear implants: A review of methods and interpretation," J. Acoust. Soc. Am. **131**, 2209–2224.

Miller, C. A., Robinson, B. K., Woo, J., and Hu, N. (**2010**). "Physiological and anatomical changes in the auditory nerve fibers of chronically deaf cats," ARO **33**, 910.

Nelson, D. A., and Donaldson, G. S. (**2001**). "Psychophysical recovery from single-pulse forward masking in electric hearing," J. Acoust. Soc. Am. **109**, 2921–2933.

Nelson, D. A., and Donaldson, G. S. (**2002**). "Psychophysical recovery from pulse-train forward masking in electric hearing," J. Acoust. Soc. Am. **112**, 2932–2947.

Oxenham, A. J., and Moore, B. C. (**1994**). "Modeling the additivity of nonsimultaneous masking," Hear. Res. **80**, 105–118.

Pfingst, B. E., Colesa, D. J., Hembrador, S., Kang, S. Y., Middlebrooks, J. C., Raphael, Y., and Su, G. L. (**2011**). "Detection of pulse trains in the electrically stimulated cochlea: Effects of cochlear health," J. Acoust. Soc. Am. **130**, 3954–3968.

Ramekers, D., Versnel, H., Strahl, S. B., Klis, S. F., and Grolman, W. (**2015**). "Recovery characteristics of the electrically stimulated auditory nerve in deafened guinea pigs: Relation to neuronal status," Hear. Res. **321**, 12–24.

Shannon, R. V. (**1990**). "Forward masking in patients with cochlear implants," J. Acoust. Soc. Am. **88**, 741–744.

Smith, R. L., and Brachman, M. L. (**1982**). "Adaptation in auditory-nerve fibers: A revised model," Biol. Cybern. **44**, 107–120.

Stypulkowski, P. H., and van den Honert, C. (**1984**). "Physiological properties of the electrically stimulated auditory nerve. I. Compound action potential recordings," Hear. Res. **14**, 205–223.

Westerman, L. A., and Smith, R. L. (**1984**). "Rapid and short-term adaptation in auditory nerve responses," Hear. Res. **15**, 249–260.

Wilson, B. S., Finley, C. C., Lawson, D. T., and Zerbi, M. (**1997**). "Temporal representations with cochlear implants," Am. J. Otol. **18**, S30–34.

Zhou, N., Kraft, C. T., Colesa, D. J., and Pfingst, B. E. (**2015**). "Integration of pulse trains in humans and guinea pigs with cochlear implants," J. Assoc. Res. Otolaryngol. **16**, 523–534.

Zhou, N., and Pfingst, B. E. (**2014**). "Relationship between multipulse integration and speech recognition with cochlear implants," J. Acoust. Soc. Am. **136**, 1257–1268.

Zhou, R., Abbas, P. J., and Assouline, J. G. (**1995**). "Electrically evoked auditory brainstem response in peripherally myelin-deficient mice," Hear. Res. **88**, 98–106.